Inorg. Chem. **2004**, *43*, 282–289

Synthesis and Structure of $Ca_{18}Li_5In_{25.07}$: A Novel Intergrowth of Li-Centered In_{12} Icosahedral Clusters and Electron-Precise Zintl Layers

Jiang-Gao Mao,[1] Joanna Goodey, and Arnold M. Guloy*

Department of Chemistry and Texas Center for Superconductivity, University of Houston, Houston, Texas 77204-5641

Received May 29, 2003

A new ternary polar intermetallic, $Ca_{18}Li_5In_{25.07}$, was obtained from high-temperature reactions of the elements in welded Nb tubes. Its crystal structure, established by single-crystal X-ray diffraction, was found to crystallize in the orthorhombic space group *Cmmm* (No. 65). Unit cell parameters are $a = 9.9151(6)$ Å, $b = 26.432(2)$ Å, and $c = 10.2116(6)$ Å; $Z = 2$. The structure of $Ca_{18}Li_5In_{25.07}$ features two distinct types of indium anionic layers. An "electron-deficient" layer is made up of Li-centered In_{12} icosahedra that are interconnected by bridging planar In_4 units and In atoms. A second In_3^{5-} layer is an electron-precise Zintl layer formed by fused four-, five-, and six-membered rings of three- and four-bonded indium atoms. The two distinct layers are alternately stacked and linked into a complex three-dimensional network. Vacancies are observed to occur only at the In_{12} icosahedral and the bridging indium units within the "electron-deficient" layers. Magnetic property measurements indicate that $Ca_{18}Li_5In_{25.07}$ exhibits temperature-independent paramagnetism consistent with metallic behavior. Band structure calculations were performed to elucidate the role of defects and vacancies in the electronic structure of the electron-deficient "metallic" Zintl phase.

Introduction

Intermetallic phases formed between the elements of group 13 (triels) with one or more of the electropositive alkali or alkaline earth metals often show a rich variety of very complicated and often unique structures.[2] More importantly, the smooth transition of electronic properties from semiconducting Zintl phases to normal intermetallic compounds that occurs within trielides and tetrelides provides a fertile area to search for materials with novel electronic structures and chemical bonding. This offers unique opportunities in investigating relationships between crystal structure, chemical bonding, and physical properties. In this context, the Zintl concept provides an effective and useful starting point to rationalize chemical bonding and electronic properties of materials in the border between metals and nonmetals.[3] Our recent investigations aim to probe the validity of the Zintl concept in rationalizing the synthesis and chemical bonding of complex intermetallic compounds on the Zintl border. This has led to the successful synthesis and description of $SrCa_2In_2Ge$, that contains novel $[In{=}In{-}Ge]^{6-}$ chains, analogous to and isoelectronic with the allyl anion chain $[CH{=}CH{-}CH_2]_\infty$.[4] Further exploratory work led to the discovery of the unusual compound $Ca_5In_9Sn_6$ with an unprecedented Zintl-intermetallic intergrowth structure.[5] It features the anionic $[In_3]^{5-}$ fragments analogous and isoelectronic with the simplest aromatic cyclopropenium molecule. Recently, our exploratory work has resulted in the synthesis of the novel transition metal polar intermetallic phase Ba_2NiSi_3 that features a unique bonding between Ni and Si_3 ring fragments in a chain analogous to metallocenes.[6] The resulting discovery of novel intermetallic π-systems emphasizes the validity of the Zintl approach to rationalize electron-deficiency in intermetallics along the Zintl border in terms of formation of unsaturated or multiple bonds.

* Author to whom correspondence should be addressed. E-mail: Aguloy@uh.edu.

(1) Current address: State Key Laboratory of Structural Chemistry, Fujian Institute of Research on the Structure of Matter, Chinese Academy of Sciences, Fuzhou 350002, P. R. China.

(2) (a) Von Schnering, H. G. *Angew. Chem., Int. Ed. Engl.* **1981**, *20*, 33. (b) Schäfer, H. *Annu. Rev. Mater. Sci.* **1985**, *15*, 1.

(3) (a) Miller, G. In *Chemistry, Structure and Bonding of Zintl Phases and Ions*; Kauzlarich, S., Ed.; VCH Publisher: New York, 1996; pp 1−55. (b) Nesper, R. *Angew. Chem., Int. Ed. Engl.* **1991**, *30*, 789.

(4) Xu, Z.; Guloy, A. M. *J. Am. Chem. Soc.* **1997**, *119*, 10541.

(5) Xu, Z.; Guloy, A. M. *J. Am. Chem. Soc.* **1998**, *120*, 7349.

(6) Goodey, J.; Mao, J.-G.; Guloy, A. M. *J. Am. Chem. Soc.* **2000**, *122*, 10478.

10.1021/ic034594t CCC: $27.50
Published on Web 12/06/2003

"Electron deficiency" in polar intermetallic compounds of group 13 (trielide) post-transition elements is usually demonstrated by the formation of multicenter 2-electron bonds that leads to the formation of isolated and linked cluster units. The tendency of polar intermetallic trielides to form borane-like clusters is illustrated by the extensive studies on a wide variety of novel trielide cluster compounds which can be rationalized in terms of Wade's rules as in the boranes.[7,8] Thallium exhibits predominantly isolated clusters, and gallium forms many network structures usually constructed through bonding of recognizable deltahedral clusters, in addition to a number of isolated cluster units. On the other hand, indium provides a mix of both network and discrete deltahedral cluster examples and the best examples of heterometal-centered clusters. Among a number of cluster units, the icosahedral geometry has been found to be common for all three triels.[7] Removal of one and two icosahedral vertices produces its derivative *nido* and *arachno* species, respectively. In the solid state this can also be achieved by the formation of vacancies (defects) at specific cluster vertices.[8] An illustrative example is the binary phase $Na_7In_{11.76}$ that features a novel *closo*-In_{16} elongated icosioctahedral and *nido*-In_{11} icosahedral units.[9] The 10-bonded *nido*-In_{11} icosahedra exhibit fractional occupancy at one vertex effectively generating a proportional amount of *arachno*-In_{10} cluster units. Application of the Zintl electron counting scheme and Wade's cluster bonding description, taking into account the vacancies, show that the cluster compound essentially exhibits a closed-shell count. The observed fractional occupancy on one of the icosahedral cluster vertices, resulting in the formation of both *nido*-In_{11} and *arachno*-In_{10} in 5:3 proportions, thereby satisfies the necessary electronic requirement and is clearly "a recognized means of adaptation" for solid-state cluster compounds.[9]

Herein we report a result of our investigations on the synthesis and chemical bonding of complex polar intermetallic phases along the border between electron-precise Zintl phases and normal intermetallics. Studies on the complex chemical system containing group 13 elements, alkali earth metals, and lithium led to the discovery of an unusual intermetallic compound, $Ca_{18}Li_5In_{25.07}$. The compound reveals a new intergrowth structure between "electron-deficient" cluster and "electron-precise" Zintl layers. The "electron-deficient" cluster layer features Li-centered In_{12} icosahedra interconnected (8-exo-bonds) through planar In_4 fragments and individual bridging In atoms. A novel electron-precise In_3^{5-} Zintl layer, made up 3- and 4-bonded indium linked into 4-, 5-, and 6-membered indium rings, is similar and isoelectronic with the $GaSb_2^-$ anionic layer found in the Zintl phase $KGaSb_2$.[10]

(7) (a) Corbett, J. D. In *Chemistry, Structure and Bonding of Zintl Phases and Ions*; Kauzlarich, S., Ed.; VCH Publishers: New York, 1996. (b) Corbett, J. D. *Angew. Chem., Int. Ed.* **2000**, *39*, 670 and references therein.

(8) (a) Belin, C.; Tillard-Charbonnel, M. *Prog. Solid State Chem.* **1993**, *22*, 59. (b) Burdett, J. K.; Canadell, E. *J. Am. Chem. Soc.* **1990**, *112*, 7207. (c) Tillard-Charbonnel, M.; Manteghetti, A.; Belin, C. *Inorg. Chem.* **2000**, *39*, 1684.

(9) Sevov, S. C.; Corbett, J. D. *Inorg. Chem.* **1992**, *31*, 1895.

(10) Cordier, G.; Ochmann, H. Z. *Kristallogr.* **1991**, *197*, 297.

Experimental Section

Syntheses. The title compound was initially obtained from the high-temperature reactions of the pure elements (Ca pieces, 99.99%; Li ribbons, 99.9%; In shots, 99.9999%; Ge powder, 99.9999%) according to molar ratio of 2:1:2:1 in welded Nb tubes within an evacuated quartz jacket. The reactions were performed at 1000 °C for 7 days with prior heating under dynamic vacuum at 300 °C for 1 day, and then were allowed to cool slowly to room temperature. As a general precaution, all sample manipulations were done within a purified argon atmosphere glovebox that had a moisture level of less than 0.1 ppm. After proper structure characterization and microprobe analysis, the air and moisture sensitive compound $Ca_{18}Li_5In_{25.07}$ was synthesized in high yields from reactions of stoichiometric mixtures of the pure elements at 800 °C. All diffraction lines observed in the X-ray powder patterns could be indexed according to a calculated diffraction pattern based on the single-crystal refinement results.

Crystal Structure Determination. Single crystals were selected from reaction product and sealed within thin-walled glass capillaries under argon atmosphere. A block-shaped shiny black single crystal with approximate dimensions of 0.06 × 0.08 × 0.10 mm was mounted on Siemens SMART 1K CCD (Mo Kα radiation, graphite monochromator). Accurate cell constants were indexed from 39 reflections chosen from 60 frames collected with a 10-s exposure per frame. A hemisphere of data (1271 frames at detector distance of 5 cm) was collected by the narrow-frame method with scan widths of 0.30° in ω and an exposure time of 40 s per frame, up to $2\theta_{max} = 56.0°$ at 293(2) K. The first 50 frames were re-collected at the end of data collection to assess the stability of the crystal, and the decay in intensity was later found to be less than 1%. A total of 8351 reflections were measured, of which 1744 reflections were independent and 1454 reflections with $I > 2\sigma(I)$ were considered observed. The data were corrected for Lorentz factor, polarization, air absorption, and absorption due to variations in the path length through the detector faceplate. Empirical absorption corrections based on SADABS were also applied.[11]

The space group was determined to be *Cmmm* (No. 65) based on the observed systematic absences and counting statistics. The crystal structure was solved using direct methods using SHELXTL that revealed all calcium and indium atom positions. The lithium atom positions were subsequently located from difference Fourier calculations. All atomic positional coordinates, anisotropic thermal parameters for Ca and In atoms, and the isotropic thermal parameters for all lithium atoms were refined by least-squares methods (84 variables; $S = 1.074$, R1 = 0.031 and wR2 = 0.081 for observed data).[11] During refinement, we found that five indium positions (In(5), In(6), In(7), In(8), and In(9)) were partially occupied. This was indicated by abnormally high thermal parameters, and their site occupancy factors were refined accordingly. The occupancy factors for all indium atoms were refined. Resulting occupancies for In(1), In(2), In(3), and In(4) are more than 98% and were subsequently considered fully occupied. The resulting chemical composition based on structural refinement is $Ca_{18}Li_5In_{25.072(5)}$. Final least squares refinement indicated that the difference Fourier map was essentially featureless with residual peaks of 1.31 and −2.10 e Å^{-3} that are 0.84 and 0.51 Å from In(8) and In(4) atoms, respectively. X-ray diffraction data collection parameters and final structural refinement results are summarized in Table 1.

(11) Sheldrick, G. M. *Program SADABS*; 1995. Sheldrick, G. M. *SHELXTL*, version 5.03; Siemens Analytical X-ray Instructuments: Madison, WI, 1995. Sheldrick, G. M. *SHELX-96 Program for Crystal Structure Determination*; Universität Göttingen: Göttingen, 1996.

Table 1. Crystallographic Data and Structure Refinement Results for $Ca_{18}Li_5In_{25.07}$

empirical formula	$Ca_{18}Li_5In_{25.07}$
formula weight	3634.68
crystal system	orthorhombic
space group	*Cmmm* (No. 65)
unit cell dimensions	
a	9.9151(6) Å
b	26.432(2) Å
c	10.2116(6) Å
volume	2676.2(3) Å^3
Z	2
density (calculated)	4.511 g/cm^3
absorption coefficient	12.284 mm^{-1}
F(000)	3207
max and min transmission factors	1.0−0.735
crystal dimensions	0.06 × 0.08 × 0.10 mm
2θ range for data collection	3 to 56.0
index ranges	$-12 \le h \le 12$, $-31 \le k \le 33$, $-8 \le l \le 13$
reflections collected	8351
independent reflections	1744 [R(int) = 0.0354]
observed reflections ($I > 2\sigma(I)$)	1454
refinement method	full-matrix least-squares on F^2
data/restraints/parameters	1743/0/84
GOF on F^2	1.074
final *R* indices (observed data)	R1 = 0.0313, wR2 = 0.0813
R indices (all data)	R1 = 0.0410, wR2 = 0.0947
largest diff peak and hole	1.314 and −2.099 e Å^{-3}

Table 2. Atomic Coordinates and Equivalent Thermal Parameters (Å^2 × 10^3) for $Ca_{18}Li_5In_{25.07}$

atom	site	*x*	*y*	*z*	occupancy	*U*(eq)[a]
Ca(1)	4i	0	0.2050(1)	1	1	15(1)
Ca(2)	4k	1/2	1/2	0.2777(4)	1	29(1)
Ca(3)	4i	0	0.4286(1)	0	1	14(1)
Ca(4)	8q	0.1928(2)	0.3160(1)	1/2	1	13(1)
Ca(5)	16r	0.3043(1)	0.3863(1)	0.2060(1)	1	14(1)
Li(1)	8n	0	0.3118(5)	0.227(1)	1	6(3)
Li(2)	2c	0	1/2	1/2	1	18(7)
In(1)	8n	0	0.4066(1)	0.3480(1)	1	11(1)
In(2)	8p	0.1556(1)	0.3156(1)	1	1	14(1)
In(3)	8m	1/4	1/4	0.7783(1)	1	16(1)
In(4)	8n	1/2	0.2901(1)	0.6465(1)	1	22(1)
In(5)	4j	1/2	0.3898(1)	1/2	0.794(5)	19(1)
In(6)	8o	0.1552(1)	1/2	0.2548(1)	0.681(3)	14(1)
In(7)	4i	1/2	0.5735(1)	0	0.751(5)	20(1)
In(8)	4g	0.2845(2)	1/2	0	0.685(5)	22(1)
In(9)	8q	0.2526(2)	0.4441(1)	1/2	0.472(3)	16(1)

[a] *U*(eq) is defined as one-third of the trace of the orthogonalized $\mathbf{U}_{ij}$ tensor.

The atom coordinates and the relevant bond lengths and bond angles are listed in Tables 2 and 3, respectively. More details on the crystallographic studies as well as atom thermal parameters are given in the Supporting Information.

The chemical compositions of several single crystals were also quantitatively analyzed by microprobe WDS (wavelength dispersive spectrometer) with appropriate standards. Results indicate a uniform composition, the presence of Li, and a Ca:In atomic ratio of 0.720-(1):1. This value is in excellent agreement with the results from single-crystal structure refinement. Since accurate analysis for lithium based on X-rays is difficult, lithium composition was confirmed by the high yield synthesis of the compound in reactions with nominal stoichiometry about the ideal value. The nearly constant lattice parameters (within 2σ) with variation of the lithium composition indicate the narrow homogeneity range of the lithium stoichiometry. Moreover, bulk composition of a sample composed of several single crystals of the title compound was determined using atomic absorption analysis, and results are consistent with the refined chemical composition. Accurate lattice parameters were obtained by careful indexing of the experimental X-ray diffraction patterns with the theoretical diffraction pattern obtained from the single-crystal structure refinement results, using NBS Si as an internal standard.

Band Structure Calculations. The electronic structure of the title compound was calculated using the LCAO (tight-binding) approximation within the extended-Hückel theory (EHT).[12] Atomic orbital and energy parameters were employed as before.[4,5,13] Consistent with the premise of the Zintl concept, the electropositive metals Ca and Li in $Ca_{18}Li_5In_{25.07}$ donate their electrons to the anionic In network. Consequently, theoretical calculations were performed on the relevant two-dimensional substructures and the complete three-dimensional network of In_{30}^{41-} with idealized occupancies. Sufficiently large k-point sets (50), selected from the irreducible wedge in the Brillouin zone, were used in all calculations and integrations for Mulliken populations, overlap populations, total energies, densities of states (DOS), and crystal orbital overlap populations (COOP) curves. The atomic orbital and energy parameters were employed as shown in Table 2.

Magnetic Property Characterization. Magnetic susceptibility experiments were performed using an Oxford Instruments Maglab 9T vibrating sample magnetometer (VSM). The measurements were taken on two single-phase powder samples over the temperature range 4−300 K, at magnetic field strengths of 0.5 and 1.0 T. Each of the polycrystalline powder samples was pressed into 1/8 in. diameter pellets that were fastened to a standard sample holder with Teflon tape. All manipulations and handling of samples were performed under argon atmosphere to avoid oxidation of the air-sensitive compound. The magnetic susceptibility data were initially corrected for diamagnetic contributions from the sample holder and ion cores.

Results and Discussion

Crystal Structure. The compound $Ca_{18}Li_5In_{25.07}$ represents a new structure type in both Zintl chemistry and intermetallic crystal structures. The rather complex crystal structure, shown in Figure 1, can be described as an alternate stacking of two types of layers, namely, a defect "electron-deficient" cluster layer and an "electron-precise" Zintl layer. The main structural feature of the "electron-deficient" cluster layer is the In_{12} icosahedral cluster. The In_3^{5-} layered network is considered electron precise.

The In_{12} icosahedral unit, as shown in Figure 2, is represented by In(1), In(6), and In(9). The In−In cluster distances in the In_{12} icosahedral unit, that range from 2.955 to 3.109 Å, are very close to those found for the *closo*-In_{12} icosahedron in $A_3Na_{26}In_{48}$ (A = K, Rb, Cs).[14] The In_{12} icosahedron is centered by the Li(2) atom, with Li−In separations ranging from 2.908(2) Å to 2.939(1) Å. A number of centered thallium polyhedra and In_{10} polyhedron have been reported wherein the trielide clusters are either centered by alkali metal or late transition metal atoms.[7] The Li-centered In_{12} icosahedra in $Ca_{18}Li_5In_{25.07}$ is 8-*exo*-bonded and linked to form a layered network of clusters. The normal two-center-two-electron *exo*-bonds (2.842(2) and 2.900(1) Å) are slightly shorter than the multicenter-two-electron *intra*-cluster In−In bonds in the In_{12} icosahedral units.

(12) (a) Hoffmann, R. *J. Chem. Phys.* **1963**, *39*, 1397. (b) Whangbo, M.-H.; Hoffmann, R. *J. Am. Chem. Soc.* **1978**, *100*, 6093.
(13) Mao, J.-G.; Xu, Z.; Guloy, A. M. *Inorg. Chem.* **2001**, *40*, 4472.
(14) Sevov, S. C.; Corbett, J. D. *Inorg. Chem.* **1993**, *32*, 1612.

Table 3. Selected bond lengths (Å) and angles (deg) for $Ca_{18}Li_5In_{25.07}$

Ca(1)−In(2)	2×	3.306(3)	Ca(1)−In(2)	2×	3.4585(9)	Ca(1)−In(3)	4×	3.561(1)
Ca(1)−In(4)	2×	3.6126(8)	Ca(1)−In(7)		3.475(3)	Ca(2)−In(5)	2×	3.693(3)
Ca(2)−In(6)	2×	3.427(1)	Ca(2)−In(7)	2×	3.438(4)	Ca(2)−In(8)	2×	3.551(3)
Ca(2)−In(9)	4×	3.654(3)	Ca(3)−In(1)	2×	3.6012(8)	Ca(3)−In(2)	2×	3.360(3)
Ca(3)−In(6)	4×	3.564(2)	Ca(4)−In(1)	2×	3.434(2)	Ca(4)−In(3)	2×	3.383(1)
Ca(4)−In(4)	2×	3.462(2)	Ca(4)−In(4)	2×	3.709(2)	Ca(4)−In(5)		3.616(2)
Ca(3)−In(8)	2×	3.394(2)	Ca(4)−In(9)		3.437(2)	Ca(4)−In(4)	2×	3.462(2)
Ca(5)−In(1)		3.390(1)	Ca(5)−In(2)		3.177(2)	Ca(5)−In(3)		3.647(1)
Ca(5)−In(4)		3.536(2)	Ca(5)−In(5)		3.576(1)	Ca(5)−In(6)		3.386(1)
Ca(5)−In(7)		3.052(2)	Ca(5)−In(8)		3.673(1)	Ca(5)−In(9)		3.408(2)
Li(1)−In(1)		2.794(14)	Li(1)−In(2)	2×	2.786(14)	Li(1)−In(3)	2×	2.969(8)
Li(1)−In(4)		2.986(14)	Li(2)−In(1)	4×	2.9168(7)	Li(2)−In(6)	4×	2.939(1)
Li(2)−In(9)	4×	2.908(2)	In(1)−In(1)		3.104(1)	In(1)−In(6)	2×	3.0617(8)
In(1)−In(9)	2×	3.109(1)	In(2)−In(2)		3.085(1)	In(2)−In(3)	2×	3.0014(7)
In(3)−In(4)	2×	3.0135(6)	In(4)−In(4)		2.991(2)	In(4)−In(5)		3.029(1)
In(5)−In(9)	2×	2.842(2)	In(6)−In(6)		3.077(2)	In(6)−In(8)		2.900(1)
In(6)−In(9)	2×	3.064(1)	In(7)−In(8)	2×	2.888(2)	In(9)−In(9)		2.955(3)

In(1)−In(1)−In(9)	2×	60.06(2)	In(6)−In(1)−In(1)	2×	108.12(2)
In(6)−In(1)−In(6)		60.34(4)	In(6)−In(1)−In(9)	2×	107.62(4)
In(6)−In(1)−In(9)	2×	59.54(3)	In(9)−In(1)−In(9)		107.34(5)
In(3)−In(2)−In(3)		97.90(3)	In(3)−In(2)−In(2)	2×	108.18(1)
In(2)−In(3)−In(2)		82.10(3)	In(2)−In(3)−In(4)	2×	106.47(2)
In(2)−In(3)−In(4)	2×	112.98(2)	In(4)−In(4)−In(3)	2×	116.55(2)
In(4)−In(3)−In(4)		126.91(4)	In(3)−In(4)−In(3)		110.68(3)
In(3)−In(4)−In(5)	2×	121.77(2)	In(4)−In(4)−In(5)		60.42(2)
In(9)−In(5)−In(9)		119.30(8)	In(9)−In(5)−In(4)	4×	116.07(3)
In(4)−In(5)−In(4)		59.17(4)	In(8)−In(6)−In(1)	2×	120.08(3)
In(1)−In(6)−In(1)		107.54(4)	In(1)−In(6)−In(9)	2×	107.05(4)
In(8)−In(6)−In(9)	2×	126.42(5)	In(1)−In(6)−In(9)	2×	61.00(3)
In(9)−In(6)−In(9)		57.67(5)	In(8)−In(6)−In(6)		116.24(4)
In(1)−In(6)−In(6)	2×	59.83(2)	In(9)−In(6)−In(6)	2×	108.38(3)
In(8)−In(7)−In(8)		95.42(6)	In(7)−In(8)−In(7)		84.58(6)
In(7)−In(8)−In(6)	4×	109.09(2)	In(6)−In(8)−In(6)		127.53(7)
In(5)−In(9)−In(9)		120.35(4)	In(5)−In(9)−In(6)	2×	121.05(3)
In(9)−In(9)−In(6)	2×	61.17(3)	In(6)−In(9)−In(6)		109.64(5)
In(5)−In(9)−In(1)	2×	122.28(5)	In(9)−In(9)−In(1)	2×	108.61(3)
In(6)−In(9)−In(1)	2×	107.93(5)	In(6)−In(9)−In(1)	2×	59.46(3)
In(1)−In(9)−In(1)		59.89(4)			

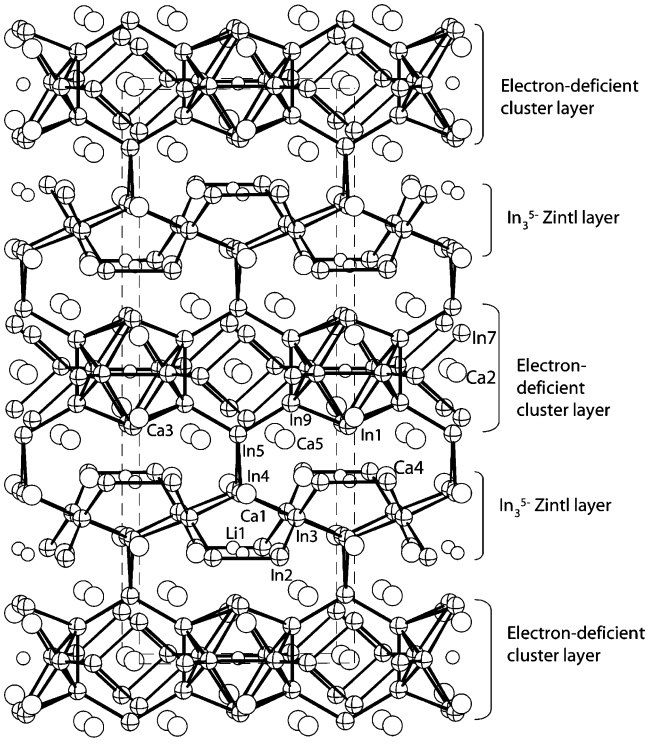

Figure 1. The [001] view of the crystal structure of $Ca_{18}Li_5In_{25.07}$. Ca, In, and Li atoms are represented as large (empty), medium (crossed), and small (empty) spheres, respectively. In−In bonds are drawn. The interlayer In4−In5 distance is 3.029(1) Å.

The 8-*exo*-bonded In_{12} icosahedra are linked through bridging indium atoms (In(5) and In(8)) forming a two-

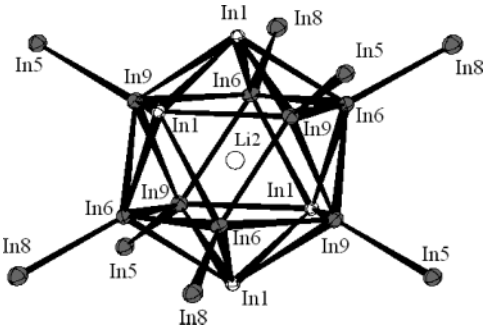

Figure 2. ORTEP representation of the 8-*exo*-bonded Li-centered In_{12} icosahedron in $Ca_{18}Li_5In_{25.07}$. Thermal ellipsoids of indium are drawn at 50% probability, and important distances (Å) are listed as follows: In1−In1, 3.104(1); In1−In6, 3.0617(8); In1−In9, 3.109(1); In6−In6, 3.077(2); In6−In9, 3.064(1); In9−In9, 2.955(3); In5−In9, 2.842(2); In6−In8, 2.900(1). In sites that exhibit vacancies are shaded for clarity.

dimensional layer along the ⟨010⟩ plane as illustrated in Figure 3. Adjacent In_{12} cluster units are bridged, through *exo*-bonds, along the *a* and *c* axes by In(5) and In(8), respectively. Adjacent bridging In(8) atoms along the *a*-axis are further bridged by In(7). The fragment formed by the linking of In(8) and In(7) can be considered as unique bridging unit of the "electron-deficient" cluster layer—planar In_4 rhomboids. Within each In_4 rhomboid unit, the In−In bond length is 2.888(2) Å and the In−In−In angles are 84.58(6) and 95.42(6)° at In(8) and In(7), respectively. Each In_4 unit effectively links four In_{12} icosahedral units through two In(8) atoms. The geometry of the resulting $(In_{12})_4In_4$ unit, wherein the In(8) atom is four-bonded and the In(7) atom is

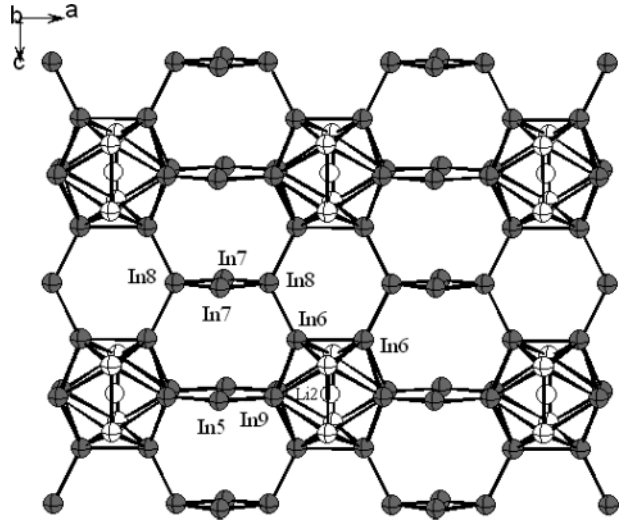

Figure 3. The [010] view of the cluster layer in $Ca_{18}Li_5In_{25.05}$ that features In_{12} icosahedra interconnected by bridging atoms and In_4 fragments. Relevant distances are as follows: In7−In8, 2.888(2) Å; In6−In8, 2.900-(1) Å; In5−In9, 2.842(2) Å. In sites that exhibit vacancies are shaded for clarity.

two-bonded, is that of an edge-shared dimer of tetrahedra with In(7) acting as the two-bonded bridge between In(8), and the vertices of the In_{12} icosahedra as the terminal ligands. The dimer of edge-shared tetrahedra is a common structural feature among many Zintl phases, for example, the $[Sn_2Sb_6]^{10-}$ Zintl anion found in Na_4KSnSb_3.[15,16]

The unusual crystal structure of $Ca_{18}Li_5In_{25.07}$ is also marked by the occurrence of vacancies or defects that are found only within atom positions that make up the "electron-deficient" cluster layer. These defects are preferentially located at *exo* bonded icosahedral vertices (In(6), 0.681(3); and In(9), 0.472(3)) and all of the bridging indium atoms (In(5), 0.794(5); In(7), 0.751(5); and In(8), 0.695(5)). Formation of vacancies (defects) is commonly observed among electron-deficient cluster phases of gallium and indium. These vacancies are manifested as fractional occupancies of atom positions at the vertices of the Tr_{12} icosahedra or at bridging atom sites.[8] It has also been shown that the defects and vacancies observed among the trielide cluster compounds have an electronic origin associated with an electron counting scheme that optimizes the occupancy of cluster bonding levels.[8]

The other interesting structural component in the compound $Ca_{18}Li_5In_{25.07}$ is an anionic layer, In_3^{5-}, as shown in Figure 4a. The electron-precise layer is made up of three- and four-bonded indium atoms (In(2), In(3), and In(4)) that form 4-, 5-, and 6-membered rings. The Zintl layer can be built from a familiar unit—a pair of edge-shared tetrahedra. The edge-shared tetrahedron is represented by In(2) − common edge; In(3) − centers of the tetrahedra and In(4) − terminal corners = In_8 units. The edge-shared tetrahedral units are further linked through common vertices (In(4)) to form a chain of corner-shared In_8 units along the *a*-axis.

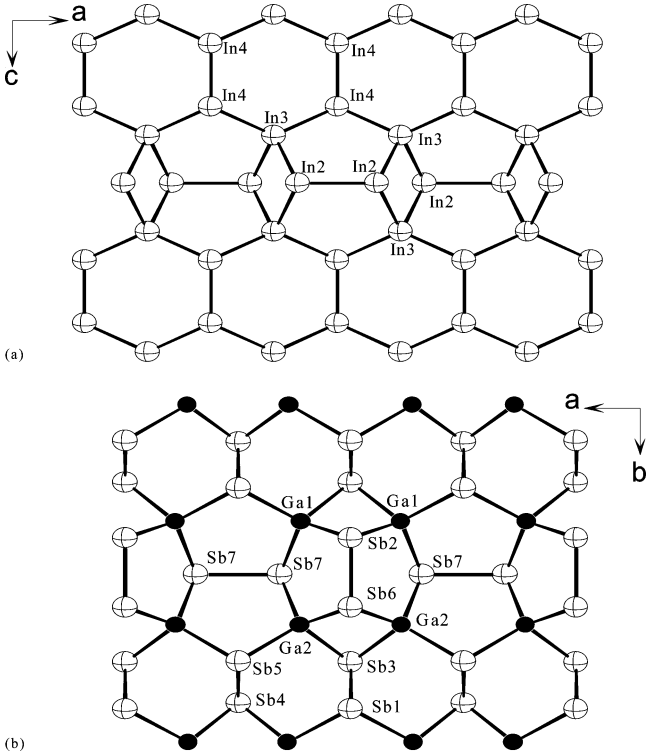

Figure 4. (a). The [010] view of the $[In_3]^{5-}$ Zintl layer in $Ca_{18}Li_5In_{25.07}$. Important In−In distances (Å): In2−In2, 3.085(1); In2−In3, 3.0014(7); In3−In4, 3.0135(6); In4−In4, 2.991(2). (b) Corresponding view of the $[GaSb2]^-$ Zintl anion layer in $KGaSb_2$.

Subsequent formation of bonds between the bridging In(2) atoms of adjacent In_8 units leads to the formation of pentagonal rings, ultimately resulting in chains of edge-shared planar five-membered rings. Edge-shared pentagonal rings are familiar structural units of zeolitic and clathrate-like network Zintl phases.[13,17] The layer is finally formed by linking parallel chains via bonds between nearest neighboring vertices of adjacent chains. The joining of the parallel chains of five-membered rings results in the formation of hexagonal indium rings. The six-membered rings form a nominal chain of edge-shared hexagons along the *a*-axis.

The resulting Zintl anionic layered network, $[In_2(In_2In_{4/2})]^{10-} = In_3^{5-}$, closely resembles the structure of the isoelectronic $[GaSb_2]^-$ layer found in the Zintl phase $KGaSb_2$,[10] as shown in Figure 4b. In $KGaSb_2$, each four-bonded Ga atom is coordinated to four Sb (3-bonded) atoms and the $GaSb_4$ tetrahedra are linked in a manner that also results in the formation of 4-, 5-, and 6- membered rings, each ring containing two Ga atoms.[10] In deriving the $Ca_{18}Li_5In_{25.07}$ structure from $KGaSb_2$ it would be necessary to replace both Ga and Sb atoms with In, and applying a 90° rotation alternately on a pair of adjacent edge-shared indium pentagons. The difference between the related layer structures lies on the orientation of the pentagons with respect to the rows of hexagon rings. In $Ca_{18}Li_5In_{25.07}$, each 4-membered indium ring is linked to four 5-membered rings via edge sharing and with two indium hexagons through sharing corners (see Figure 4a). This arrangement is a slight modification of that

(15) Klein, J.; Eisenmann, B. *Z. Kristallogr.* **1991**, *196*, 213.
(16) Eisenmann, B; Cordier, G. In *Chemistry, Structure and Bonding of Zintl Phases and Ions*; VCH Publishers: New York, 1996; p 61.
(17) Corbett, J. D. In *Chemistry, Structure and Bonding of Zintl Phases and Ions*; VCH Publishers: New York, 1996; p 139.

found in $[GaSb_2]^-$, wherein each 4-membered ring is linked through common edges with two pentagons and two 6-membered rings, and linked through common vertices with two indium pentagons. It should be noted that the In_3^{5-} Zintl anion layer in $Ca_{18}Li_5In_{25.07}$ differs from the isoelectronic unit of isolated or "molecular" In_3^{5-} anions (cyclopropenium-like) found in $Ca_5In_9Sn_6$.[5] The In−In distance in the In_3^{5-} layer ranges from 3.001 to 3.085 Å, comparable to the In−In distances found in In_{12} cluster, and is slightly longer than the *exo* In−In bonds of the cluster layer.

Combining the two different types of anionic layers finally leads to the complex three-dimensional anionic network of indium in $Ca_{18}Li_5In_{25.07}$. The "electron-deficient" cluster and "electron-precise" Zintl layers are alternately stacked along the *b* axis and linked through In−In single bonds between the cluster-bridging atoms In(5) of the cluster layer and the terminal vertices, In(4), of the edged-shared tetrahedral In_8 unit. The complete crystal structure is shown in Figure 1. The formation of interlayer In−In bonds effectively makes In(5) and In(4) four-bonded. The interlayer In(5)−In(4) bond length is 3.029(1) Å, which is comparable to the In−In distances within the Zintl In_3^{5-} layer. However, the interlayer In−In bond is slightly longer than the *exo*-bonds of the In_{12} icosahedron, consistent with a layered description. The difference may lie on the matrix effects associated with the occurrence of vacancies in the cluster layer and the difference in the sizes of the cation spacers.

The calcium and lithium atoms of $Ca_{18}Li_5In_{25.07}$ effectively act as "spacers" in the crystal structure. Calcium atoms, Ca(1), Ca(3), Ca(4), and Ca(5), form a nominal double layer of calcium atoms between the two different layers, and exhibit high coordination numbers (11, 10, 10, and 9, respectively). The remaining calcium atoms, Ca(2), lie within the cluster layer and exhibits 12-fold coordination. The Ca(2) atoms occupy the cavities formed by the bridging In_4 units and In12 clusters of the cluster layer and effectively act as spacers between the icosahedra within the cluster layer. As previously mentioned, the Li(2) atoms are located at the center of In_{12} icosahedral units. The remaining lithium atoms Li(1), located at the periphery of the Zintl layer, exhibit a normal 6-fold coordination. The nearest neighbors of Li(1) are five In atoms of a 5-membered ring in the Zintl layer and one In(1) atom from a neighboring In_{12} cluster. The coordination geometry around each Li(1) can be described as that of a pentagonal pyramid. All Ca−In distances, ranging from 3.052(2) to 3.693(3) Å, and Li−In distances, ranging from 2.786(12) to 2.986(14) Å, are comparable to those found in related polar intermetallics and Zintl phases.[4,5,7,13]

Based on the crystal structure, the chemical bonding in $Ca_{18}Li_5In_{25.07}$ is interesting on two points. First, the title compound exhibits the structural and chemical behavior of solid-state cluster compounds of alkali metal trielides with icosahedral units, including the presence of vacancies and nonstoichiometry. On the other hand, the other component of the same compound exhibits structural features and stoichiometric behavior associated with electron-precise Zintl phases. Furthermore, $Ca_{18}Li_5In_{25.07}$ features both localized

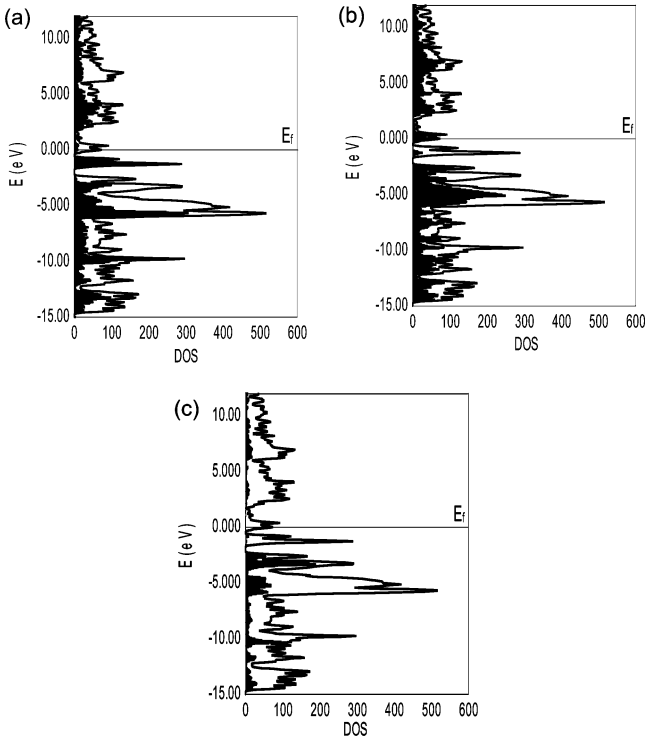

Figure 5. Relevant densities-of-states (DOS) curves showing the contribution of (a) In_{12} cluster, (b) In_3^{5-} Zintl layer, and (c) In_4 bridging units to the total DOS of $Ca_{18}Li_5In_{30}$. The Fermi level is set to 0.00 eV.

bonds between indium atoms as in $CaIn_2$ and delocalized bonds like those of indium-rich alkali metal indides.[8,9,18]

Electronic Structure. To assess chemical bonding of the title compound, and to understand a possible rationale for the preferential occurrence of defects or vacancies in the cluster layer, two- and three-dimensional band structure calculations were performed on the In_{30}^{41-} network and its component layers. In these calculations, all indium atoms were treated with ideal (100%) site occupancies. The results of the three-dimensional calculations are summarized in Figures 5 and 6. These are analyzed and related to the two-dimensional calculations performed on the component cluster and Zintl layers. The analyses of the resulting band structures indicate that the electronic structure of the three-dimensional network can be derived from a rigid band approach. Except for the increased dispersion of the bands associated with the interlayer bridging atoms, the band structure of the three-dimensional network closely resembles the combination of the electronic structures of the component layers. This is confirmed by inspection of the nature of the orbital contributions (coefficients) to the bands of the component layers.

For the electron count associated with ideal occupancies, i.e., $Ca_{18}Li_5In_{30}$, the states immediately below the Fermi level are mainly contributions from the strongly antibonding states of the In_{12} icosahedra, and some nonbonding states related to the bridging indium atoms of the cluster layer. The unoccupied states immediately above the Fermi level are mostly derived from antibonding states of the In_3^{5-} Zintl layer. The relevant indium bonding levels associated with the Zintl layer lie significantly below the Fermi level (∼−4

(18) Mao, J.-G.; Guloy, A. M. *J. Alloys Compd.* **2001**, *322*, 135.

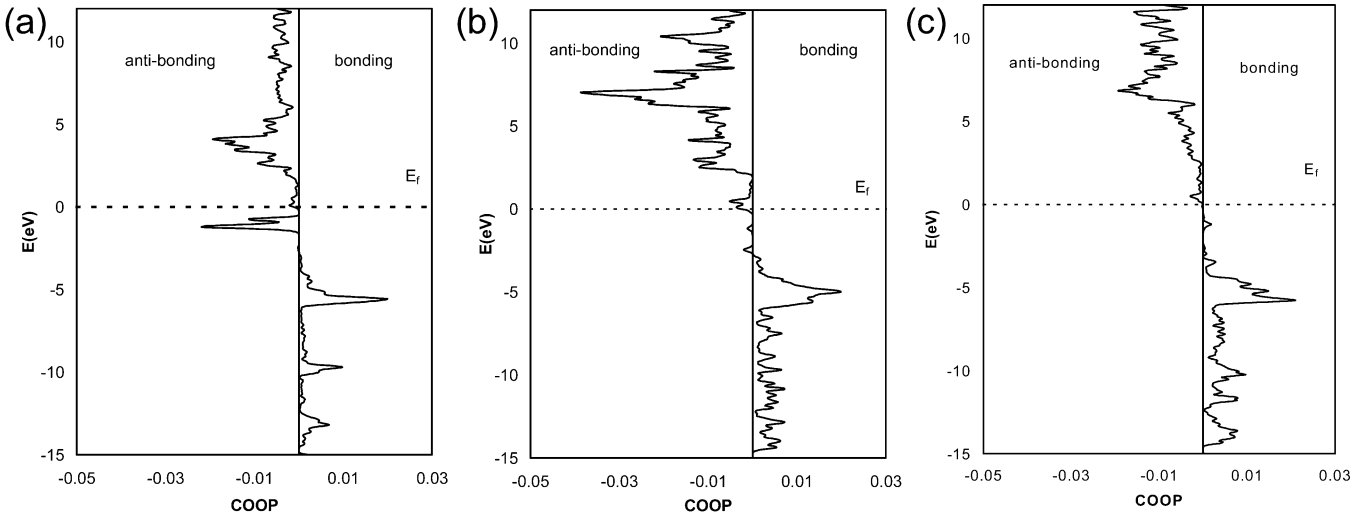

Figure 6. Crystal orbital overlap population (COOP) curves of relevant In−In interactions in $Ca_{18}Li_5In_{30}$: (a) In−In (In_{12} cluster bonds); (b) In−In (bonds in In_3^{5-}); and (c) In(4)−In(5) (interlayer bonds).

eV), and below the antibonding states of the "electron-deficient" cluster layers. This implies that the occupied bonding states of the "electron-precise" Zintl layers are stabilized to lower energies (more electronegative) and are electronically "isolated" from the states of the "electron-deficient" cluster layers. One can then argue that, at the idealized "defect-free" electron count, the In−In cluster bonds are weakened due to the strongly antibonding nature of the highest occupied states. Hence, one can expect that bonding interactions in the "electron-rich" $Ca_{18}Li_5In_{30}$ are enhanced by "oxidization" or a decrease in the electron count, as well as by a decrease in the available antibonding states.[19] These conditions can readily be achieved in $Ca_{18}Li_5In_{25.07}$ by the formation of vacancies at the In_{12} icosahedra and the bridging In atom sites. Consequently, the vacancies of the indium network are preferentially located at the "electron-deficient" cluster layers that account for the antibonding states near the Fermi level. The effects of the nonstoichiometry are consistent with the above picture. The formation of defects allows for the expected decrease in electron count, tantamount to the removal of some cluster electronic states. Hence, the introduction of vacancies in the "electron-deficient" cluster layer significantly lowers the Fermi level, and the optimization of the In−In interactions within the In_{12} icosahedral units of the cluster layer is generally approached. The electronic effects of defects and vacancies on the remaining In−In bonds in the Zintl $[In_3]^{5-}$ layers are expected to be negligible, leaving the optimized bonding states of the anionic Zintl layer essentially intact.

A complete and quantitative electron counting scheme that takes into account all electronic effects of vacancies on the electronic structure of $Ca_{18}Li_5In_{25.07}$ is difficult due to the need to consider a multitude of possible permutations of modeling the disorder. However, one can extract useful qualitative bonding explanations, based on the application of a rigid band approach, from the calculated electronic structure of complex intergrowth structures. In this manner, one can relate the structure and property of complex intermetallic structures based on electronically isolated structural components.

Magnetic susceptibility measurements on powder samples of $Ca_{18}Li_5In_{25.07}$ from 4 to 300 K indicate that the compound exhibits weak temperature-independent paramagnetism with susceptibilities of 1.4×10^{-2} emu/mol. Diamagnetic corrections due to ion cores (Ca^{2+}, Li^+, and In^{3+}) and Larmor precession of the electron pairs of the clusters were applied.[20] The observed magnetic behavior is consistent with a poor metallic behavior and can be rationalized by the possible conditions that lead to "metallic Zintl phases".[7b,21] Metallic conductivity among Zintl phases may arise from the overlap of a formally "filled" valence band with "empty" conduction bands. This is exhibited by seemingly closed-shell Zintl phases that conform to the structural motif of a corresponding electron count, as in the case of β-NaSn.[3,17] It is also interesting to note that the measured magnetic susceptibility of $Ca_{18}Li_5In_{25.07}$ is significantly larger than those previously reported for metallic alkali metal indium cluster compounds. However, the observed magnetic susceptibility is consistent and comparable with that of other "metallic" Zintl phases (poor-metals) containing Li.[22]

Intergrowth Approach to New Materials. An intergrowth approach that has been successfully used in the design of complex metal oxides can also be applied to the discovery of unusual polar intermetallics.[23] This multilayer intergrowth approach has been particularly successful in the synthesis of new layered complex oxides such as the cuprate superconductors and layered perovskites. Complex functional layered materials based on intergrowth structures of layered transition metal oxides and intermetallics have been shown

(19) Mao, J.-G.; Guloy, A. M. *J. Alloys Compd*, in press.

(20) Ashcroft, N. W.; Mermin, D. N. *Solid State Physics*; Holt, Rinehart and Winston: Philadelphia, 1976; p 649.
(21) Nesper, R. *Prog. Solid State Chem.* **1990**, *20*, 1.
(22) Xu, Z. Ph.D. Thesis, University of Houston, 1999.
(23) Brock, S. L.; Kauzlarich, S. M. *CHEMTECH* **1995**, *25*, 18. Guloy, A. M.; Goodey, J. *Condens. Matter News* **1998**, *7*, 24. Cava, R. J.; Zandbergen, H. W.; Krajewski, J. J.; Siegrist, T.; Hwang, H. Y.; Batlogg, B. *J. Solid State Chem.* **1997**, *129*, 250.

to exhibit novel physical properties such as superconductivity, giant magnetoresistance (GMR), and other electronic and magnetic phenomena.[23] A similar intergrowth approach applied to polar intermetallics and Zintl phases has also been reported.[5,24] Corbett and co-workers reported several related Zintl phases in the Mg−La−Sb system based on the intergrowth of LaSb intermetallic layers and Mg_3Sb_2 Zintl layers.[24a] Also, the application of a "chemical twinning" approach to the preparation of complex yet electron-precise silicides has been described.[24b] The previously reported $Ca_5In_9Sn_6$ phase that features the In_3^{5-} cyclopropenium analogue exhibits a complex intergrowth structure of Zintl and normal intermetallic layers. More recently, a binary intermetallic, $NaSn_5$, was reported to exhibit an unusual structure that features both the covalent α-Sn and metallic β-Sn layers.[25] The title compound, $Ca_{18}Li_5In_{25.07}$, represents a new three-dimensional network in which layers of "electron-deficient" indium clusters exhibiting delocalized cluster bonding are intergrown with Zintl layers of "electron-precise" covalently bonded indium atoms. Thus, the title compound represents a class of polar intermetallics that lie at the border between delocalized bonding associated with "electron-deficient" clusters and localized bonding associated with semiconducting Zintl phases. Like in previously reported intermetallic π-systems ($SrCa_2In_2Ge$, $Ca_5In_9Sn_6$, and $BaNiSi_3$), metallic−nonmetallic intergrowth polar intermetallics emphasize the richness of the Zintl border in the synthesis of novel complex intermetallics with unusual chemical bonding. The intermetallic intergrowth approach, guided by the Zintl concept, is a simple yet useful approach to understanding the synthesis, crystal structure, and chemical bonding of complex intermetallics with novel structures and unusual bonding schemes.

Acknowledgment. Financial support for this work is provided by the National Science Foundation (CAREER Award, DMR-9733587), the Texas Center for Superconductivity and Advanced Materials at the University of Houston, and the Petroleum Research Fund administered by the American Chemical Society. This work made use of MRSEC/TCSUH Shared Experimental Facilities supported by the NSF (DMR-9632667) and the State of Texas through the TCSUH.

Supporting Information Available: X-ray crystallographic files in CIF format for the structure determination of $Ca_{18}Li_5In_{25.07}$. Tables of crystallographic data for $Ca_{18}Li_5In_{25.07}$. ORTEP views of $Ca_{18}Li_5In_{25.07}$. This material is available free of charge via the Internet at http://pubs.acs.org.

IC034594T

(24) (a) Ganguli, A. K.; Kwon, Y.-U.; Corbett, J. D. *Inorg. Chem.* **1993**, *32*, 4354. (b) Zurcher, F.; Wengert, S.; Nesper, R. *Inorg. Chem.* **1999**, *38*, 4567.

(25) Faessler, T. F. and Kronseder, C. *Angew. Chem., Int. Ed.* **1998**, *37*, 1571.